Scholars Journal of Agriculture and Veterinary Sciences OPEN ACCESS
Abbreviated Key Title: Sch J Agric Vet Sci
ISSN 2348–8883 (Print) | ISSN 2348–1854 (Online)
Journal homepage: https://saspublishers.com

Spectral Separability Analysis of Mango and Litchi Canopies Using Sentinel-2 Surface Reflectance Data in Gopalganj District, India

Ankit Kumar Yadav[1*], Dr. Udai Raj[2]

[1]Project Scientist, Remote Sensing Applications Centre, Lucknow
[2]Scientist-SE, Remote Sensing Applications Centre, Lucknow

DOI: https://doi.org/10.36347/sjavs.2026.v13i04.002 | **Received:** 04.02.2026 | **Accepted:** 11.03.2026 | **Published:** 30.05.2026

***Corresponding author:** Ankit Kumar Yadav
Project Scientist, Remote Sensing Applications Centre, Lucknow

Abstract **Original Research Article**

Accurate identification of perennial fruit orchards is essential for strengthening horticultural statistics, precision management and policy planning in eastern India, where mango (*Mangifera indica* L.) and litchi (*Litchi chinensis* Sonn.) constitute major fruit-based livelihoods. In Bihar, orchard inventories remain largely field-based, and quantitative evaluation of species-level spectral separability using medium-resolution satellite data is limited. This study assesses the spectral distinctness of mango and litchi canopies using single-date Sentinel-2 Level-2A surface reflectance imagery acquired on 14 May 2025 over Gopalganj district, Bihar. Eight bands (B2, B3, B4, B5, B6, B7, B8 and B11) were analysed, with 20 m bands resampled to 10 m, and reflectance statistics were derived from 40 digitised training polygons per species. Multivariate Bhattacharyya distance and its Jeffries–Matusita (JM) transformation were used to quantify separability. The resulting JM value of 1.9588 (0–2 scale) indicates excellent separability and very low expected classification confusion. Band-wise decomposition shows that visible wavelengths dominate separability, with B4 (red) contributing 27.29%, B2 (blue) 20.30%, B3 (green) 18.51% and B5 (red-edge) 15.90%, while SWIR1 (B11) contributes 10.32% and near-infrared bands contribute comparatively less. These patterns are consistent with the spectral reflectance curves, where litchi exhibits higher reflectance in the visible region and mango shows stronger near-infrared scattering. The findings demonstrate that Sentinel-2 surface reflectance, particularly the visible and early red-edge bands, can effectively distinguish mango and litchi orchards in smallholder landscapes, providing a basis for operational fruit-crop mapping, orchard inventory and targeted management in subtropical agro-ecosystems.

Keywords: Spectral Separability; Jeffries–Matusita Distance; Mango; Litchi; Canopy Reflectance.

1. INTRODUCTION

Mango (*Mangifera indica* L.) and litchi (*Litchi chinensis* Sonn.) are among the most economically important fruit crops in India and play a central role in the horticultural economy of Bihar. Mango occupies a large share of the national fruit area and production, and Bihar is widely recognised for high-quality cultivars such as Zardalu and Gulabkhas. State statistics indicate that mango accounts for the largest area under fruit cultivation in Bihar, exceeding 1.6 lakh ha with production above 1.5 million tonnes in recent years (National Horticulture Board, 2001; Department of Agriculture–Horticulture, 2020). Although litchi has a narrower climatic range, Bihar contributes a dominant share of India's litchi area and production, making it the leading litchi-producing state (FAO, 1997; Jha & Sinha, 2018). Both crops support smallholder livelihoods and emerging value chains, including fresh fruit marketing and processing industries. Reliable spatial information on orchard extent and species composition is therefore essential for production estimation, flood-risk assessment in north Bihar, and planning of post-harvest infrastructure.

Conventional orchard statistics in the state rely primarily on field-based enumeration, which is labour-intensive, temporally sparse and often inconsistent across administrative scales. Satellite remote sensing offers a synoptic and repeatable alternative capable of wall-to-wall mapping. Vegetation reflectance in the visible region is governed mainly by chlorophyll absorption, while near-infrared reflectance is controlled by internal leaf structure and canopy architecture; the red-edge region captures the transition between these processes and is highly sensitive to vegetation biophysical properties (Lin *et al*., 2019; Ustin & Jacquemoud, 2020; Bayle *et al*., 2019). The Sentinel-2 MultiSpectral Instrument, with visible, red-edge, NIR and SWIR bands at 10–20 m resolution, has demonstrated strong capability for crop and vegetation

classification (Immitzer *et al*., 2019; Qiu *et al*., 2017). However, quantitative evidence on species-level spectral separability of perennial orchard crops using single-date surface reflectance data remains limited, particularly in smallholder landscapes.

Although separability metrics such as the Bhattacharyya and Jeffries–Matusita distances are widely used to evaluate class distinctness prior to classification (Swain & King, 1973; Bruzzone *et al*., 1995), explicit reporting of their magnitude and band-wise contributions for fruit-tree species is rare. This limits objective assessment of optimal band selection and operational feasibility for orchard mapping. The present study addresses this gap by evaluating the spectral separability between mango and litchi canopies in Gopalganj district, Bihar, using single-date Sentinel-2 Level-2A surface reflectance data. Specifically, it characterises canopy reflectance behaviour across key spectral bands, quantifies overall class separability using multivariate Bhattacharyya and Jeffries–Matusita distances, and assesses the relative contribution of individual bands to the separability measure, thereby providing methodological evidence for species-level orchard mapping in subtropical agro-ecosystems.

1. STUDY AREA

Gopalganj district is located in the north-western part of Bihar, India, and forms part of the alluvial plains of the middle Gangetic basin. The district lies roughly between 26.2–26.8° N latitude and 83.8–84.6° E longitude, bordered by the Gandak River and adjoining districts of Saran and Siwan. It has a predominantly flat topography with elevations around 70–80 m above mean sea level and is intersected by numerous distributaries and flood channels (Department of Agriculture–Horticulture, 2020).

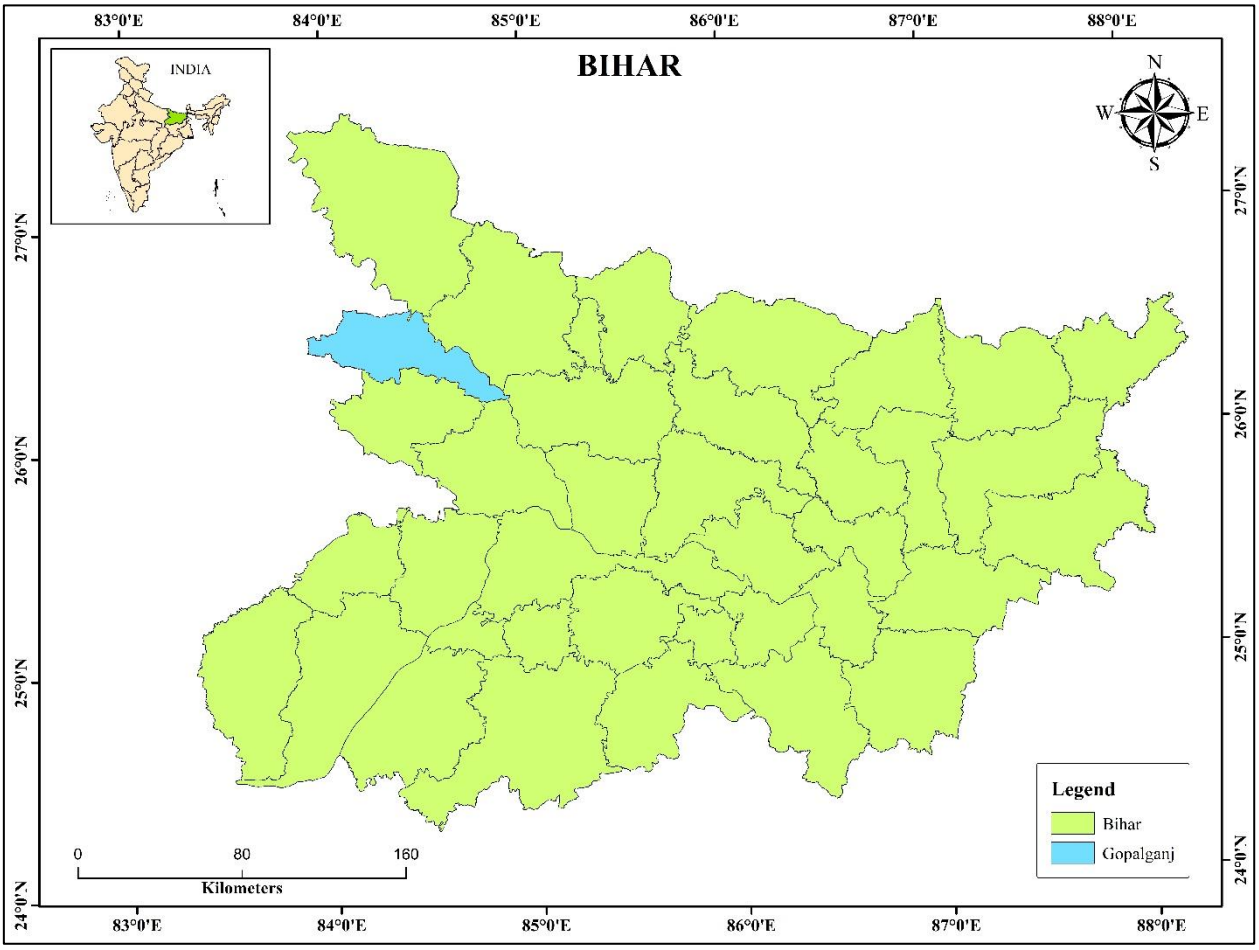

Figure 1: Map of the Study Area

The climate is humid subtropical, characterised by a hot summer, a monsoon season from June to September and a cool winter. Mean annual rainfall is approximately 1000–1200 mm, with the majority received during the southwest monsoon (All Commerce Journal, 2024). Temperature ranges from about 8–10 °C in winter to 35–40 °C in pre-monsoon months. Such conditions favour a diverse cropping pattern dominated by rice–wheat rotations, pulses and oilseeds, along with substantial horticultural production.

Mango and litchi orchards are interspersed with agricultural fields and homestead gardens across the district. Bihar's status as a leading producer of both mango and litchi implies that districts such as Gopalganj contribute significantly to the state's horticultural output (National Horticulture Board, 2001; Jha & Sinha, 2018). Mango orchards often consist of mature trees with broad, evergreen canopies, whereas litchi orchards form more compact canopies with dense foliage and distinct phenology, including early flushing and flowering that precede mango in many locations (FAO, 1997). The mixture of orchards and seasonal crops, combined with small parcel sizes typical of eastern India, presents a challenging but relevant context for evaluating spectral separability at 10 m spatial resolution.

3. DATA AND METHODOLOGY

The overall methodological framework adopted in this study is illustrated in Figure 2. The workflow integrates satellite data processing, training sample generation, statistical feature extraction, and multivariate separability analysis in a structured sequence. Sentinel-2 Level-2A surface reflectance imagery constituted the primary dataset and underwent systematic pre-processing, including band extraction, spatial harmonisation, compositing, and reflectance scaling. In parallel, representative mango and litchi orchard polygons were delineated through visual image interpretation and on-screen digitisation to generate reliable training samples.

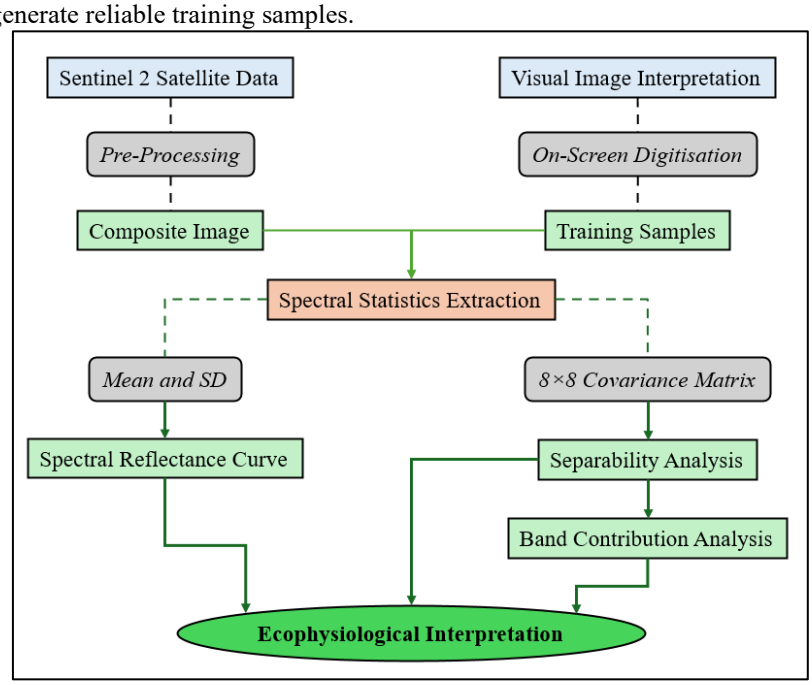

Figure 2: Methodological framework adopted for spectral separability analysis of mango and litchi canopies

The processed multi-band composite and digitised training samples were subsequently combined for ROI-based spectral statistics extraction. Class-wise mean reflectance, standard deviation, and 8×8 covariance matrices were computed to characterise within-class variability and inter-band relationships. These statistical descriptors formed the basis for multivariate separability analysis using Bhattacharyya and Jeffries–Matusita distance measures. Finally, band contribution analysis and spectral reflectance curve evaluation supported ecological interpretation of species-specific canopy behaviour.

The following subsections describe each methodological component in detail.

3.1 Satellite Data

A Sentinel-2B Level-2A product (surface reflectance) for tile T45RTK, acquired on 14 May 2025, covering Gopalganj district was used for the analysis. Level-2A product provides bottom-of-atmosphere reflectance after atmospheric correction, including aerosol and water vapour effects in 13 spectral bands, and is widely recommended for multi-date or quantitative reflectance studies (SNAP Sentinel-2 MSI Reader, 2023). The acquisition date corresponds to late pre-monsoon conditions, when both mango and litchi orchards maintain dense foliage and minimal cloud contamination over the study area.

Eight spectral bands were selected based on their relevance to vegetation and availability at 10–20 m resolution (Table 1). These bands collectively span the visible, red-edge, NIR and SWIR domains that are known to capture differences in chlorophyll absorption, canopy structure and water content (Lin *et al*., 2019; Bayle *et al*., 2019). The 20 m bands were resampled to match the 10 m grid of the visible and NIR bands, enabling multivariate analysis at a uniform spatial resolution.

Table 1: Sentinel-2 MultiSpectral Instrument (MSI) bands used in this study

Band	Spectral region	Central wavelength (µm)	Description	Spatial Resolution (m)
B2	Visible blue	0.49	Blue	10
B3	Visible green	0.56	Green	10
B4	Visible red	0.665	Red	10
B5	Red-edge 1	0.705	Vegetation red-edge	20
B6	Red-edge 2	0.74	Vegetation red-edge	20
B7	Red-edge 3	0.783	Vegetation red-edge	20
B8	Near-infrared (NIR)	0.842	NIR	10
B11	Short-wave IR (SWIR)	1.61	SWIR-1	20

3.2 Pre-processing

Standard preprocessing steps were applied to the Level-2A product prior to analysis. First, individual bands corresponding to B2, B3, B4, B5, B6, B7, B8 and B11 were extracted from the Sentinel-2 SAFE archive using ESA SNAP and a geographic information system environment (SNAP Sentinel-2 MSI Reader, 2023).

Second, all 20 m bands (B5, B6, B7 and B11) were resampled to 10 m using bilinear interpolation, which preserves smooth spatial transitions and is widely used for Sentinel-2 band harmonisation (Zhang *et al*., 2025; SNAP Sentinel-2 MSI Reader, 2023). This step ensured co-registration and consistent pixel size across the selected bands.

Finally, the stack of eight bands was combined into a single multi-band raster representing surface reflectance. Reflectance values in the Level-2A product are stored as scaled digital numbers (DN). A surface reflectance scaling factor of $\rho = \frac{\text{DN}}{10000}$ was applied to convert all bands to physical reflectance between 0 and 1 prior to analysis.

3.3 Training Sample Collection

Training samples representing pure orchard canopy pixels were delineated through visual interpretation of high-resolution reference imagery available in Google Earth (Google LLC, 2024), following a field survey in which GPS was used to record the latitude and longitude of different orchards (Figure 3).

(a) **(b)**

Figure 3: Field photographs of representative orchard canopies in Gopalganj district: (a) mango orchard; (b) litchi orchard

A total of 40 mango orchard polygons and 40 litchi orchard polygons were digitised across Gopalganj district, ensuring adequate representation of the major orchard clusters while avoiding very small or mixed orchards. The polygons were delineated to encompass contiguous tree crowns, while excluding obvious mixed pixels along orchard edges, roads, ponds, and field boundaries (Figure 4). Only well-established orchards exhibiting clear canopy expression on the Sentinel-2 imagery were selected. Mixed pixels were intentionally avoided in order to minimise within-class spectral heterogeneity attributable to non-orchard components.

The digitised polygons were overlaid on the 10 m reflectance layer-stacked composite image and converted into Region of Interest (ROI) masks for subsequent extraction of spectral statistics. This procedure yielded 980 Mango pixels and 927 Litchi pixels for subsequent statistical analysis.

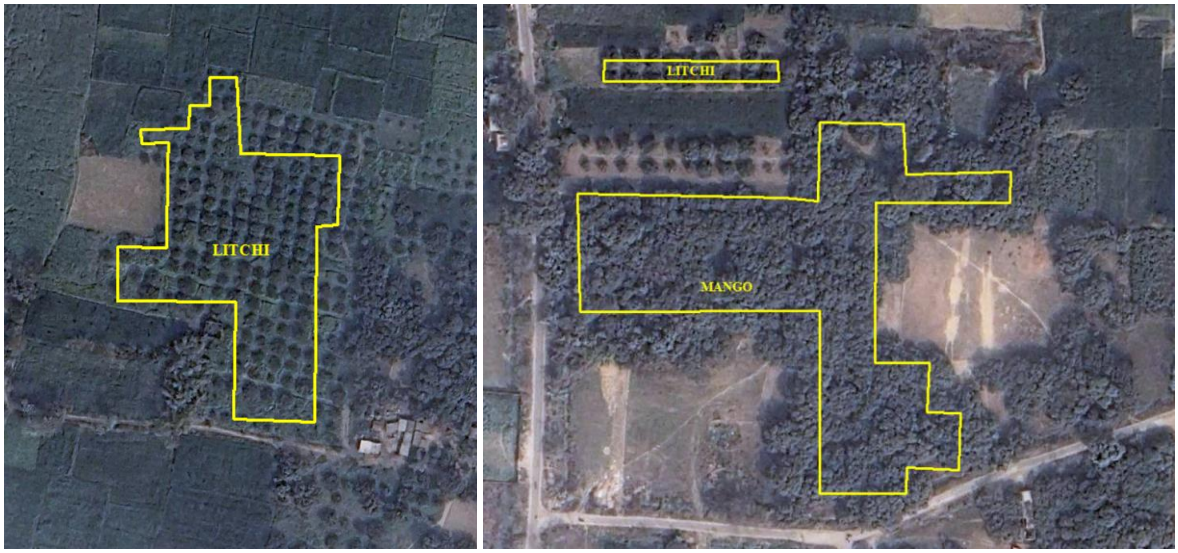

Figure 4: Digitised training polygons representing mango and litchi orchards in Gopalganj district

3.4 Spectral Statistics Extraction

For each orchard class (Mango and Litchi), training pixels within the delineated ROIs were used to extract per-pixel DN values for the eight selected Sentinel-2 bands. Sampling and signature extraction were performed using the ROI, zonal statistics, and signature analysis tools in ArcGIS 10.8.

For each class and band, descriptive statistics of minimum, maximum, mean, standard deviation, and sum were computed from the DN values. Using the same training pixels, 8×8 band-to-band covariance matrices were generated separately for Mango and Litchi to characterise within-class spectral variability and inter-band relationships.

All DN-based statistics were subsequently rescaled to surface reflectance units by applying the Sentinel-2 scale factor (1/10000). This conversion yielded mean reflectance and standard deviation values per band in physically interpretable reflectance units. Data tabulation, verification, and matrix handling were performed in Microsoft Excel.

The class-wise covariance matrices were later used for the computation of Bhattacharyya and Jeffries–Matusita distance measures to assess spectral separability.

Finally, spectral reflectance curves were constructed by plotting mean reflectance values against the central wavelength of each band for both classes. These curves visually support the separability analysis by identifying spectral regions that most effectively distinguish mango and litchi orchard canopies.

3.5 Separability Analysis

Spectral separability between Mango and Litchi orchards was quantified using the Bhattacharyya distance and the Jeffries–Matusita distance, which are widely used in remote sensing feature selection and classification studies (Swain & King, 1973; Bruzzone *et al*., 1995; Sen *et al*., 2022). Both measures assume that class conditional distributions can be approximated by multivariate normal densities.

Let $\mu_1$and $\mu_2$be the mean vectors for Mango and Litchi, and $\Sigma_1$and $\Sigma_2$their respective covariance matrices. The average covariance matrix is

$$\Sigma = \frac{1}{2}(\Sigma_1+\Sigma_2).$$

The Bhattacharyya distance B between the two classes is defined as (Swain & King, 1973; Bruzzone *et al*., 1995):

$$B = \frac{1}{8}(\mu_1 - \mu_2)^T\Sigma^{-1}(\mu_1 - \mu_2) + \frac{1}{2}\ln\left(\frac{\det\Sigma}{\sqrt{\det\,\Sigma_1 \det\,\Sigma_2}}\right). \quad (1A)$$

The first term represents a Mahalanobis-type distance between class means and the second term accounts for differences in the covariance structures.

Given two classes with mean vectors μ_1 and μ_2 and covariance matrices Σ_1 and Σ_2 in an n-dimensional feature space (here $n = 8$), the Bhattacharyya distance B was computed as

$$B = \frac{1}{8}(\mu_1 - \mu_2)^T \left(\frac{\Sigma_1 + \Sigma_2}{2}\right)^{-1} (\mu_1 - \mu_2) + \frac{1}{2}\ln\left(\frac{\det\left(\frac{\Sigma_1 + \Sigma_2}{2}\right)}{\sqrt{\det(\Sigma_1)\det(\Sigma_2)}}\right). \quad (1B)$$

This formulation combines the Mahalanobis distance between class means and a term accounting for differences in class covariance structures (Swain & King, 1973).

The Jeffries–Matusita distance JM was then obtained through the exponential transformation

$$JM = 2(1 - e^{-B}). \quad (2)$$

This transformation maps the Bhattacharyya distance to a bounded range of 0 to 2, providing an interpretable measure of class separability (Swain & King, 1973; Bruzzone *et al*., 1995). Values close to 0 indicate strong overlap between class distributions, whereas values approaching 2 indicate near-complete separability and correspond to low theoretical Bayes classification error.

The Semi-Automatic Classification Plugin (SCP) in QGIS was supplied with the per-band mean vectors, standard deviations, and covariance matrices for Mango and Litchi. Using Equations (1B) and (2), the plugin computed the overall Bhattacharyya and Jeffries–Matusita distances, along with the relative contribution of each band to total separability. This is further discussed in Section 4.3.

In addition to the full 8-band separability assessment, a band-wise contribution analysis was performed. For each band, the incremental change in Bhattacharyya distance resulting from its inclusion was calculated, and individual contributions were normalised to sum to 100%. This analysis identifies the spectral regions that most strongly enhance class discrimination and supports feature selection for classification.

4. RESULTS

4.1 Spectral Statistics and Signature Behaviour

Rescaled mean surface reflectance and standard deviation values for Mango and Litchi canopies across the eight selected Sentinel-2 bands are presented in Table 2.

In the visible region (B2–B4), Litchi consistently exhibits higher mean reflectance than Mango. The largest difference occurs in the red band (B4), where Litchi reflectance exceeds Mango by approximately 0.0566 reflectance units. This pattern indicates stronger attenuation of visible radiation in Mango canopies, potentially associated with greater chlorophyll absorption or denser foliage structure.

At the first red-edge band (B5), Litchi remains brighter than Mango, with a difference of approximately 0.0401. However, from B6 to B8 (red-edge to NIR), the relationship reverses. Mango reflectance becomes higher than Litchi by approximately 0.0228–0.0397 reflectance units, suggesting stronger multiple scattering within Mango canopies and possible structural differences in leaf arrangement or internal leaf properties. The spectral crossover between B5 and B6 marks the transition where declining chlorophyll absorption gives way to increased near-infrared scattering.

In the SWIR1 band (B11), Litchi again exhibits higher reflectance than Mango (difference = 0.0453), indicating differences in canopy moisture content, leaf biochemical composition, or soil background influence.

Table 2: Mean Sentinel-2 surface reflectance and standard deviation for mango and litchi canopies (rescaled values)

Band	Wavelength region	Mango (Mean)	Litchi (Mean)	Mango (SD)	Litchi (SD)
B2	Blue	0.1128	0.1474	0.0107	0.0157
B3	Green	0.1563	0.1884	0.0088	0.0160
B4	Red	0.1382	0.1948	0.0157	0.0229
B5	Red-edge 1	0.2162	0.2563	0.0136	0.0259
B6	Red-edge 2	0.3621	0.3394	0.0208	0.0227
B7	Red-edge 3	0.4120	0.3745	0.0279	0.0246
B8	NIR	0.4171	0.3775	0.0334	0.0292
B11	SWIR1	0.3293	0.3746	0.0238	0.0392

Standard deviation values show that Litchi displays greater within-class variability in B2–B5 and B11, whereas Mango exhibits slightly higher variability in B6–B8. This band-dependent variability suggests differences in canopy heterogeneity and structural complexity between the two orchard types.

4.2 Spectral Reflectance Curve

The mean reflectance values in Table 2 were plotted as a function of the central wavelength of each band to generate spectral reflectance curves for both orchard classes. Both species exhibit the typical vegetation signature characterised by low reflectance in the visible region, a sharp increase across the red edge, a high reflectance plateau in the NIR, and reduced reflectance in the SWIR (Figure 5).

The curves confirm that Litchi is brighter in the visible and SWIR regions, whereas Mango shows stronger reflectance in the central NIR. The intersection near the red-edge region highlights this transition and underscores the diagnostic importance of red-edge and NIR bands for orchard species discrimination.

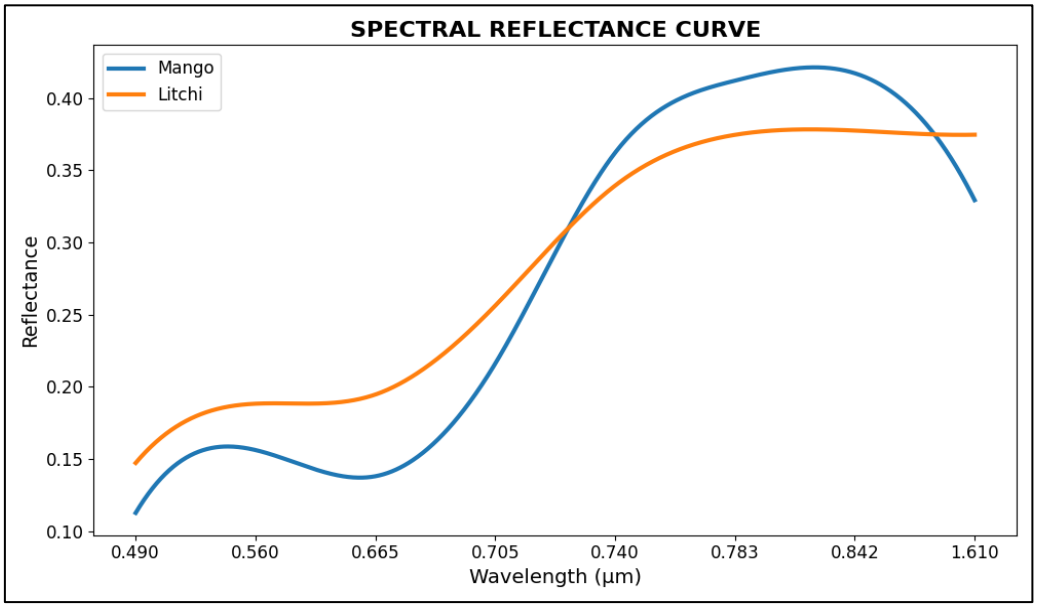

Figure 5: Spectral reflectance curves for Mango and Litchi orchards derived from rescaled mean Sentinel-2 band reflectance (B2–B8, B11)

Overall, the magnitude and shape differences in the spectral curves support the statistical separability analysis presented in the subsequent section.

4.3 Jeffries–Matusita Separability

Using the full 8-band mean vectors and covariance matrices derived from the training samples, the Bhattacharyya distance between the mango and litchi spectral distributions was computed as approximately 3.8833. Applying the transformation $JM = 2(1 - e^{-B})$ resulted in a Jeffries–Matusita distance of 1.9588. The computed separability metrics are summarised in Table 3.

Table 3: Bhattacharyya and Jeffries–Matusita separability metrics between Mango and Litchi Canopies

Metric	Value
Bhattacharyya Distance	3.8833
JM Distance (0-√2)	1.3996
JM Distance (0-2)	1.9588
Separability Quality	EXCELLENT

In remote sensing applications, JM values greater than 1.9 (on the 0–2 scale) are generally interpreted as indicating excellent class separability, with very low expected classification confusion (Swain & King, 1973; Bruzzone *et al*., 1995). As shown in Table 3, the obtained JM value of 1.9588 lies close to the theoretical upper bound of 2, indicating near-complete statistical separability between the two orchard types.

The magnitude of the JM distance suggests that, under the acquisition and sampling conditions considered, Mango and Litchi canopies occupy largely non-overlapping regions in the 8-dimensional spectral feature space. Because the JM

transformation saturates as separability increases, values approaching 2 represent an asymptotic limit corresponding to minimal Bayes classification error.

Therefore, the derived JM value confirms that Sentinel-2 surface reflectance data acquired on 14 May 2025 provide strong discriminatory capability between Mango and Litchi orchards.

4.4 Band Contribution Analysis

Decomposition of the Bhattacharyya distance into per-band components reveals that separability is dominated by the visible and early red-edge bands. The relative contributions of each band to the total separability are summarized in Table 4.

Table 4: Per-band contribution to Bhattacharyya-based separability between mango and litchi canopies

Band	Spectral region	Bhattacharyya component	Contribution (%)
B4	Red	3.4165	27.29
B2	Blue	2.5417	20.30
B3	Green	2.3172	18.51
B5	Red-edge 1	1.9912	15.90
B11	SWIR1	1.2919	10.32
B7	Red-edge 3	0.4293	3.43
B8	NIR	0.3782	3.02
B6	Red-edge 2	0.1545	1.23

The dominance of B4, B2 and B3 indicates that differences in visible reflectance, largely driven by chlorophyll absorption and leaf surface properties, are the primary determinants of class separation. The substantial contribution of B5 underscores the importance of the early red-edge region, where the slope of the reflectance curve transitions from red absorption to NIR scattering. By contrast, the central NIR bands (B6–B8) provide only modest additional separability, reflecting the relative similarity of canopy internal structure between the two orchard species. The SWIR1 band contributes meaningfully, likely capturing differences in canopy and soil moisture status or structural water absorption.

5. DISCUSSION

5.1 Eco-physiological Controls on Visible and Red-Edge Reflectance

The high Jeffries–Matusita distance obtained in this study can be interpreted in the light of eco-physiological differences between mango and litchi canopies and the spectral sensitivities of Sentinel-2 bands. Visible reflectance of tree canopies is principally controlled by leaf pigment composition, especially chlorophylls and carotenoids, as well as by leaf surface properties and background effects. Litchi leaves typically exhibit a lighter green colour (Figure 6) compared with the deep green of many mango cultivars (Figure 7), reflecting differences in pigment concentration and leaf age distribution within the canopy (FAO, 1997; Jha & Sinha, 2018).

Higher visible reflectance in litchi bands B2–B4 is consistent with comparatively lower chlorophyll absorption or a greater proportion of sunlit leaf surfaces. The strong contribution of the red band (B4) to separability indicates that small differences in chlorophyll absorption are effectively captured at 10 m resolution. Such sensitivity is well documented in studies exploring red-edge vegetation indices, where combinations of red and red-edge bands enhance sensitivity to chlorophyll variation and phenological change (Lin *et al*., 2019; Lin *et al*., 2022). The substantial importance of B5 in the band-contribution analysis further suggests that the position and steepness of the red-edge are distinct between mango and litchi, reflecting species-specific differences in pigment profiles, leaf mesophyll structure and canopy layering.

Figure 6: Litchi leaves showing lighter green coloration and comparatively thinner lamina

Figure 7: Mango leaves exhibiting darker green pigmentation and thicker, glossier leaf surface

From a phenological perspective, litchi often flowers and flushes earlier in the season than mango, which can result in canopies comprising a different mixture of leaf ages around mid-May. These differences in leaf age structure influence pigment concentration and internal scattering, thereby modulating both visible and red-edge reflectance (FAO, 1997; Jha & Sinha, 2018). The single-date snapshot in this study likely captures such phenological contrasts, enhancing separability.

5.2 Limited Contribution of NIR Bands

Despite the high overall separability, the individual NIR-region bands B6–B8 contribute relatively little to the Bhattacharyya distance. Both mango and litchi are evergreen broadleaf species with dense, multi-layered canopies. Leaf internal structure and canopy architecture, which govern NIR scattering, may therefore be broadly similar, leading to comparable NIR plateau reflectance in both species. In addition, canopy-scale NIR reflectance tends to saturate at high leaf area index, reducing sensitivity to incremental differences in structure once a certain density threshold is reached, as documented in numerous vegetation studies (Bayle *et al*., 2019; Immitzer *et al*., 2019).

The observed pattern aligns with broader evidence that red-edge and visible bands can outperform NIR in separating high-biomass vegetation types, particularly when canopies are dense and structurally similar (Qiu *et al*., 2017; Lin *et al*., 2019). For feature selection, this suggests that, in orchard landscapes with dense evergreen canopies, emphasis should be placed on visible and early red-edge bands, while NIR bands may provide redundancy rather than additional discriminatory power.

5.3 Role of SWIR Reflectance

The moderate contribution of the SWIR1 band (B11) indicates that differences in water absorption features also aid discrimination. SWIR reflectance is sensitive to leaf and canopy water content, as well as to soil moisture and woody biomass, and has been widely used in drought and soil moisture indices (Gao, 1996; Liu *et al*., 2021). Litchi canopies may possess different leaf thickness or water content relative to mango, and orchard floor management practices such as irrigation, mulching or understorey crops can differentially influence SWIR signals between the two species, even where structural characteristics are similar.

In the present dataset, litchi exhibits higher SWIR reflectance than mango, suggesting relatively lower effective water absorption or greater exposure of drier background components. This difference, though less dominant than visible and red-edge contrasts, contributes meaningfully to the overall separability and may be particularly useful under conditions where visible bands are affected by haze or residual atmospheric effects.

5.4 Operational Relevance for Species-Level Orchard Mapping

The high JM distance obtained here implies that, under suitable phenological timing and atmospheric conditions, single-date Sentinel-2 surface reflectance can support robust classification of mango and litchi orchards using standard supervised algorithms. Previous work has demonstrated that Jeffries–Matusita distance correlates well with classification accuracy and serves as an effective criterion for feature selection in multispectral remote sensing (Swain & King, 1973; Bruzzone *et al*., 1995; Padma *et al*., 2014).

The band-contribution results further indicate that a reduced feature set comprising B2–B5 and B11 may capture most of the separability between the two species, offering opportunities to simplify classification models and reduce data dimensionality. This is consistent with broader findings that Sentinel-2 red-edge and SWIR bands enhance vegetation mapping, particularly when combined with visible bands (Qiu *et al*., 2017; Immitzer *et al*., 2019; Lin *et al*., 2019). For operational orchard mapping programmes in Bihar, such band selection could help streamline processing pipelines and improve model transferability.

Accurate, species-resolved orchard maps can support multiple applications, including estimation of species-specific area and productive potential, identification of vulnerable orchards in flood-prone zones, and targeting of extension interventions for cultivar replacement, pruning or disease management (Department of Agriculture–Horticulture, 2020; Jha & Sinha, 2018). In the context of emerging agri-tech initiatives in Bihar's mango sector, spatially detailed maps could also underpin digital advisory services and value-chain planning (Kumar & Mishra, 2024).

5.5 Limitations and Future Work

Several limitations of the present study should be acknowledged. First, the analysis is based on single-date imagery, capturing canopy spectral properties only at one stage of the seasonal cycle. Spectral differences between mango and litchi may vary across phenological phases; multi-temporal Sentinel-2 data could reveal additional separability or, conversely, periods of convergence. Studies using time-series vegetation indices and phenology metrics have shown improved discrimination of vegetation types compared with single-date approaches (Villa *et al*., 2021; Zhang *et al*., 2025).

Second, the training dataset comprises a limited number of polygons and does not explicitly account for intra-species variability in cultivar, age or management practices. Although the JM distance is high, separability estimates might change with larger, more diverse samples or in other districts. Third, this study focuses solely on spectral separability and does not evaluate actual classification accuracy using machine-learning or parametric classifiers. While JM provides a robust proxy for expected performance, empirical validation against independent reference data would be required for operational deployment (Swain & King, 1973; Padma *et al*., 2014).

Finally, potential confounding factors such as understory vegetation, irrigation status, soil background and small-scale topographic variation were not systematically quantified. Incorporating ancillary data such as digital elevation models, phenology metrics or textural features could enhance robustness in heterogeneous landscapes. Future research should therefore extend the analysis to multi-date imagery, larger spatial extents and explicit classification experiments, including evaluation of transferable models across seasons and nearby districts.

6. CONCLUSION

This study quantified the spectral separability between mango and litchi orchard canopies in Gopalganj district, Bihar, using single-date Sentinel-2 Level-2A surface reflectance imagery acquired on 14 May 2025. Eight bands spanning the visible, red-edge, NIR and SWIR regions were analysed using multivariate Bhattacharyya and Jeffries–Matusita distance measures derived from class-wise mean vectors and covariance matrices.

The overall Jeffries–Matusita distance of 1.9588 indicates excellent separability between mango and litchi canopies, implying that the two orchard species occupy largely distinct regions in the Sentinel-2 spectral feature space and can be discriminated reliably in classification workflows (Swain & King, 1973; Bruzzone *et al*., 1995). Band-wise analysis revealed that visible bands, particularly the red band, together with the early red-edge band B5, provide the largest contribution to separability, while central NIR bands contribute minimally and the SWIR1 band offers supplementary discrimination.

These findings align with eco-physiological expectations: litchi displays higher visible and SWIR reflectance associated with pigment and moisture differences, whereas mango exhibits stronger NIR scattering linked to canopy structural properties. The demonstrated separability confirms that Sentinel-2, despite its moderate spatial resolution, is capable of distinguishing between major orchard species in smallholder landscapes when appropriate bands and sampling strategies are employed.

From an applied perspective, the results support the development of operational orchard mapping and crop inventory systems in Bihar and similar subtropical regions. Emphasising visible and red-edge bands in feature selection and classifier design can enhance accuracy and efficiency, while the high JM value provides quantitative justification for the use of Sentinel-2 in species-level horticultural assessments (Qiu *et al*., 2017; Swain & King, 1973). Future work should incorporate multi-temporal data, larger training datasets and explicit classification accuracy assessments to generalise these conclusions and integrate them into routine horticultural monitoring programmes.

REFERENCES

1. National Horticulture Board. (2001). *Mango*. https://nhb.gov.in/report_files/mango/mango.htm
2. Department of Agriculture–Horticulture, Government of Bihar. (2020). *Model project for pack house and cold storage*. https://horticulture.bihar.gov.in/HORTMIS/ProjectBasedActivity/ProjectDocuments/ModelProject_Packhouse.pdf
3. Food and Agriculture Organization (FAO). (1997). Lychee production in India. In *Lychee production in the Asia-Pacificregion*.https://www.fao.org/4/ac684e/ac684e08.htmand https://openknowledge.fao.org/server/api/core/bitstreams/efe1d554-8e16-4468-aaf1-1ce17a62d57c/content
4. Jha, B., & Sinha, R. (2018). Litchi production, marketing and processing in Bihar and India. https://desagri.gov.in/wp-content/uploads/2024/03/2017-18-LITCHI-PRODUCTION-MARKETING-AND-PROCESSING-IN-BIHAR-AND-INDIA.pdf
5. Lin, S., Li, J., Liu, Q., Li, L., Zhao, J., & Yu, W. (2019). Evaluating the effectiveness of using vegetation indices based on red-edge reflectance from Sentinel-2 to estimate gross primary productivity. *Remote Sensing*, *11*(11), 1303. https://www.mdpi.com/2072-4292/11/11/1303
6. Ustin, S. L., & Jacquemoud, S. (2020). How the optical properties of leaves modify the absorption and scattering of energy and enhance leaf functionality. In *Remote sensing of plant biodiversity* (pp. 349-384). Cham: Springer International Publishing. https://link.springer.com/content/pdf/10.1007/978-3-030-33157-3_14.pdf
7. Bayle, A., Carlson, B. Z., Thierion, V., Isenmann, M., & Choler, P. (2019). Improved mapping of mountain shrublands using the sentinel-2 red-edge band. *Remote Sensing*, *11*(23), 2807. https://www.mdpi.com/2072-4292/11/23/2807
8. Immitzer, M., Neuwirth, M., Böck, S., Brenner, H., Vuolo, F., & Atzberger, C. (2019). Optimal input features for tree species classification in Central Europe based on multi-temporal Sentinel-2 data. *Remote Sensing*, *11*(22), 2599. https://www.mdpi.com/2072-4292/11/22/2599
9. Qiu, S., He, B., Yin, C., & Liao, Z. (2017). Assessments of sentinel-2 vegetation red-edge spectral bands for improving land cover classification. *The International Archives of the Photogrammetry, Remote Sensing and Spatial Information Sciences*, *42*, 871-874. https://isprs-archives.copernicus.org/articles/XLII-2-W7/871/2017/isprs-archives-XLII-2-W7-871-2017.html
10. Swain, P. H., & King, R. C. (1973). Two effective feature selection criteria for multispectral remote sensing. *LARS technical reports*, 39. https://docs.lib.purdue.edu/larstech/39/
11. Bruzzone, L., Roli, F., & Serpico, S. B. (1995). An extension of the Jeffreys-Matusita distance to multiclass cases for feature selection. *IEEE Transactions on Geoscience and Remote Sensing*, *33*(6), 1318-1321.
12. SNAP Sentinel-2 MSI Reader. (2023). *Import Sentinel-2 products*. https://step.esa.int/main/wp-content/help/versions/12.0.0/snap-toolboxes/eu.esa.opt.opttbx.s2msi.reader/Sentinel2Overview.html
13. Kumar, R. (2024). *Status of horticulture in Bihar*. Asian Journal of Management and Commerce, 5(2), 26–30. https://www.allcommercejournal.com/article/332/5-2-13-743.pdf
14. Zhang, M., Li, D., Li, G., & Lu, D. (2025). Vegetation classification in a subtropical region with Sentinel-2 time series data and deep learning. *Geo-Spatial Information Science*, *28*(1), 145-163. https://www.tandfonline.com/doi/pdf/10.1080/10095020.2024.2336604
15. Google LLC. (2024). *Google Earth Pro* [Computer software]. https://www.google.com/earth/

16. Sen, R., Goswami, S., Mandal, A. K., & Chakraborty, B. (2022). An effective feature subset selection approach based on Jeffries-Matusita distance for multiclass problems. *Journal of Intelligent & Fuzzy Systems*, *42*(4), 4173-4190. https://doi.org/10.3233/JIFS-202796
17. Gao, B. C. (1996). NDWI—A normalized difference water index for remote sensing of vegetation liquid water from space. *Remote sensing of environment*, *58*(3), 257-266.
18. Liu, Y., Qian, J., & Yue, H. (2021). Comprehensive evaluation of Sentinel-2 red edge and shortwave-infrared bands to estimate soil moisture. *IEEE Journal of Selected Topics in Applied Earth Observations and Remote Sensing*, *14*, 7448-7465. https://ieeexplore.ieee.org/document/9492822/
19. Padma, S., & Sanjeevi, S. (2014). Jeffries Matusita based mixed-measure for improved spectral matching in hyperspectral image analysis. *International journal of applied earth observation and geoinformation*, *32*, 138-151. https://pdfs.semanticscholar.org/d8e4/3cd7330fd9689ec24f94f187ce253e05d74e.pdf
20. Lin, S., Hao, D., Zheng, Y., Zhang, H., Wang, C., & Yuan, W. (2022). Multi-site assessment of the potential of fine resolution red-edge vegetation indices for estimating gross primary production. *International Journal of Applied Earth Observation and Geoinformation*, *113*, 102978. https://www.pnnl.gov/publications/multi-site-assessment-potential-fine-resolution-red-edge-vegetation-indices-estimating
21. Villa, P., Giardino, C., Mantovani, S., Tapete, D., Vecoli, A., & Braga, F. (2021). Mapping coastal and wetland vegetation communities using multi-temporal sentinel-2 data. *The International Archives of the Photogrammetry, Remote Sensing and Spatial Information Sciences*, *43*, 639-644.
22. Zhang, Y., Fan, Z., Yan, W., Ge, C., & Sun, H. (2025). A practical method for red-edge band reconstruction for Landsat image by synergizing Sentinel-2 data with machine learning regression algorithms. *Sensors*, *25*(11), 3570. https://www.mdpi.com/1424-8220/25/11/3570
23. Fabre, S., Elger, A., & Riviere, T. (2020). Exploitation of Sentinel-2 images for long-term vegetation monitoring at a former ore processing site. *The International Archives of the Photogrammetry, Remote Sensing and Spatial Information Sciences*, *43*, 1533-1537. https://www.int-arch-photogramm-remote-sens-spatial-inf-sci.net/XLIII-B3-2020/1533/2020/isprs-archives-XLIII-B3-2020-1533-2020.pdf
24. Raman, R. K., Singh, D. K., Sarkar, S., Singh, J., Kumar, A., Kumar, U., ... & Brahmanand, P. S. (2023). Scenario of major fruit crops in flood-prone areas in eastern India: case study of Bihar. *Erwerbs-Obstbau*, *65*(4), 1139-1151. https://link.springer.com/10.1007/s10341-022-00738-y
25. Singh, S. P., Adarsha, L. K., Nandi, A. K., & Jopir, O. (2018). Production performance of fresh Mango in India: A growth and variability analysis. *Int. J. Pure App. Biosci*, *6*(2), 935-941. http://www.ijpab.com/vol6-iss2a139.php
26. European Space Agency (ESA). (2026). Sentinel-2 mission overview. *Copernicus Data Space Ecosystem*. https://dataspace.copernicus.eu/data-collections/copernicus-sentinel-missions/sentinel-2